REPORT DOCUMENTATION PAGE

Form Approved
OMB No. 0704-0188

PLEASE DO NOT RETURN YOUR FORM TO THE ABOVE ADDRESS.

1. REPORT DATE *(DD-MM-YYYY)*	2. REPORT TYPE	3. DATES COVERED *(From - To)*
08/03/2021	Final	06/16/2018 - 06/15/2021

4. TITLE AND SUBTITLE
Conductivity Switching in Polyheterocycles

5a. CONTRACT NUMBER
N00014-18-1-2222

5b. GRANT NUMBER

5c. PROGRAM ELEMENT NUMBER

6. AUTHOR(S)
Reynolds, John Robert

5d. PROJECT NUMBER

5e. TASK NUMBER

5f. WORK UNIT NUMBER

7. PERFORMING ORGANIZATION NAME(S) AND ADDRESS(ES)
Georgia Tech Research Corporation
505 10th St. NW
Atlanta, GA 30332-0420

8. PERFORMING ORGANIZATION REPORT NUMBER

9. SPONSORING/MONITORING AGENCY NAME(S) AND ADDRESS(ES)
Office of Naval Research
875 North Randolph Street
Arlington, VA 22203-1995

10. SPONSOR/MONITOR'S ACRONYM(S)
ONR

11. SPONSOR/MONITOR'S REPORT NUMBER(S)

12. DISTRIBUTION/AVAILABILITY STATEMENT
Approved for public release; distribution is unlimited.

13. SUPPLEMENTARY NOTES

14. ABSTRACT
This work involved conjugated polymer (CP) chemistry to develop new lightweight, processable, and stable CPs with a high degree of switchability between insulating and conducting states. We synthesized and evaluated numerous electron-rich dioxythiophene (DOT) and thienothiophene (TT) polymers that incorporate both polar and non-polar side chains. This has allowed us to probe a range of properties including polarity effects, polymer/dopant interactions, solubility, and electrolyte compatibility and how these influence switchability and conductivity. In one synthesis we control biEDOT incorporation in ProDOT-based polymers (PE2) to yield materials with conductivities of 200 S/cm. Using branched oligoether side chains in PE2 structures, films with a higher average solid-state conductivity of 430 ± 60 S/cm were obtained. Through collaborations we have incorporated our materials into electrochemical switches that can modulate frequencies in the RF and microwave range (UDelaware, Mirotznik), and into carbon paper-based electrodes for flexible supercapacitors (NRL, Long and Sassin).

15. SUBJECT TERMS

16. SECURITY CLASSIFICATION OF:			17. LIMITATION OF ABSTRACT	18. NUMBER OF PAGES	19a. NAME OF RESPONSIBLE PERSON
a. REPORT	b. ABSTRACT	c. THIS PAGE		13	John R. Reynolds
					19b. TELEPHONE NUMBER *(Include area code)* 404-385-4390

INSTRUCTIONS FOR COMPLETING SF 298

1. REPORT DATE. Full publication date, including day, month, if available. Must cite at least the year and be Year 2000 compliant, e.g. 30-06-1998; xx-06-1998; xx-xx-1998.

2. REPORT TYPE. State the type of report, such as final, technical, interim, memorandum, master's thesis, progress, quarterly, research, special, group study, etc.

3. DATES COVERED. Indicate the time during which the work was performed and the report was written, e.g., Jun 1997 - Jun 1998; 1-10 Jun 1996; May - Nov 1998; Nov 1998.

4. TITLE. Enter title and subtitle with volume number and part number, if applicable. On classified documents, enter the title classification in parentheses.

5a. CONTRACT NUMBER. Enter all contract numbers as they appear in the report, e.g. F33615-86-C-5169.

5b. GRANT NUMBER. Enter all grant numbers as they appear in the report, e.g. AFOSR-82-1234.

5c. PROGRAM ELEMENT NUMBER. Enter all program element numbers as they appear in the report, e.g. 61101A.

5d. PROJECT NUMBER. Enter all project numbers as they appear in the report, e.g. 1F665702D1257; ILIR.

5e. TASK NUMBER. Enter all task numbers as they appear in the report, e.g. 05; RF0330201; T4112.

5f. WORK UNIT NUMBER. Enter all work unit numbers as they appear in the report, e.g. 001; AFAPL30480105.

6. AUTHOR(S). Enter name(s) of person(s) responsible for writing the report, performing the research, or credited with the content of the report. The form of entry is the last name, first name, middle initial, and additional qualifiers separated by commas, e.g. Smith, Richard, J, Jr.

7. PERFORMING ORGANIZATION NAME(S) AND ADDRESS(ES). Self-explanatory.

8. PERFORMING ORGANIZATION REPORT NUMBER. Enter all unique alphanumeric report numbers assigned by the performing organization, e.g. BRL-1234; AFWL-TR-85-4017-Vol-21-PT-2.

9. SPONSORING/MONITORING AGENCY NAME(S) AND ADDRESS(ES). Enter the name and address of the organization(s) financially responsible for and monitoring the work.

10. SPONSOR/MONITOR'S ACRONYM(S). Enter, if available, e.g. BRL, ARDEC, NADC.

11. SPONSOR/MONITOR'S REPORT NUMBER(S). Enter report number as assigned by the sponsoring/ monitoring agency, if available, e.g. BRL-TR-829; -215.

12. DISTRIBUTION/AVAILABILITY STATEMENT. Use agency-mandated availability statements to indicate the public availability or distribution limitations of the report. If additional limitations/ restrictions or special markings are indicated, follow agency authorization procedures, e.g. RD/FRD, PROPIN, ITAR, etc. Include copyright information.

13. SUPPLEMENTARY NOTES. Enter information not included elsewhere such as: prepared in cooperation with; translation of; report supersedes; old edition number, etc.

14. ABSTRACT. A brief (approximately 200 words) factual summary of the most significant information.

15. SUBJECT TERMS. Key words or phrases identifying major concepts in the report.

16. SECURITY CLASSIFICATION. Enter security classification in accordance with security classification regulations, e.g. U, C, S, etc. If this form contains classified information, stamp classification level on the top and bottom of this page.

17. LIMITATION OF ABSTRACT. This block must be completed to assign a distribution limitation to the abstract. Enter UU (Unclassified Unlimited) or SAR (Same as Report). An entry in this block is necessary if the abstract is to be limited.

Final Report

Conductivity Switching in Polyheterocycles
N00014-18-1-2222

John R. Reynolds
School of Chemistry and Biochemistry
School of Material Science and Engineering
Georgia Institute of Technology

reynolds@chemistry.gatech.edu

1. TECHNICAL OBJECTIVES

The goal of this project was to take advantage of the extensive expertise in conjugated polymer chemistry that our group has developed over the years and create and study known and new lightweight, processable, and stable CPs with a high degree of switchability between insulating and conducting states. Poly(3,4-ethylenedioxythiophene): poly(styrenesulfonate) (PEDOT:PSS) has reached commercial viability because of its high visible light transparency and conductivities ranging from 1 S/cm to 2,000+ S/cm using various additives and/or post-treatments. However, we wanted to move beyond the limitations of PEDOT:PSS (solubility, difficult to fully dedope, etc), and focus our efforts on solution processable polyheterocycles with strong π-π-stacking and compact dopable repeat units, sufficiently high molecular weights, and purity as needed for scalable materials that can prove relevant to commercial and defense related applications.

2. TECHNICAL APPROACH

In this program, we have synthesized and evaluated numerous electron-rich dioxythiophene (DOT) and thienothiophene (TT) polymers that incorporate both polar and non-polar side chains. This has allowed us to probe a range of properties including polarity effects, polymer/dopant interactions, solubility, and electrolyte compatibility and how these influence switchability and conductivity. We have also synthesized amine and amide derivatives to be able to probe the effects of H-bonding on transport properties, a relatively unexplored area in the conjugated polymer community due to the synthetic challenges. In addition, we have studied the effect of side chain sterics on conductivity and redox properties by varying the relative size and density of neighboring side chains, and their symmetry/asymmetry of attachment and evaluated how that affects the extent, rate, and reversibility of the doping process. The polymers we have synthesized have been thoroughly investigated by a variety of methods including differential scanning calorimetry, atomic force microscopy (AFM), and grazing-incidence wide-angle x-ray

scattering (GIWAXS) to better understand morphology effects. We have then studied the electrochemical and chemical doping processes via XPS, DC conductivity measurements, and using a host of electrochemical and spectroelectrochemical probes such as differential pulse voltammetry (DPV), cyclic voltammetry (CV), *in situ* conductance measurements, sin situ UV-vis-NIR, and electrochemical impedance spectroscopy. These measurements have all provided data to show how the structure of the polymer film can affect its onset of oxidation, charge storage capacity, conductance, doping level, and ion transport properties.

In addition to significant thrusts in in designing, synthesizing, and optimizing new polymers for high conductivity and electrochemical switchability, we have had the opportunity to combine our research efforts at Georgia Tech with those of Mark Mirotznik at the University of Delaware (UD), along with Jeff Long and Megan Sassin at the Naval Research Laboratory (NRL). These collaborations have allowed us to incorporate our materials into electrochemical switches that can modulate frequencies in the RF and microwave range (UD), and into carbon paper-based electrodes for flexible supercapacitors (NRL).

3.1 PROGRESS SUMMARY

3.1 Probing homocoupling effects in direct (hetero)arylation polymerization and its effect on conductivity

In the search for highly conductive polymers, our group has developed a solution processable copolymer PE_2 (see structure in Fig. 1a) that can be doped with a range of chemical dopants to create films with solid-state conductivities exceeding 200 S cm^{-1} under a previous ONR funded program. In this program, we have used this design motif of combining different electron-rich repeat units, where one co-monomer is functionalized with solubilizing groups and the other is minimally substituted, as this has proven to be a successful approach for obtaining materials that are easily doped and highly redox active. In addition to making backbone modification and optimizing synthetic conditions, we have also varied the solubilizing groups to better understand how side chains impact transport and switching properties.

One of our initial synthetic thrusts was to scale up the PE_2 synthesis, to better understand why PE_2 exhibits such high conductivity, and to determine if homocoupling defects resulting in an excess incorporation of biEDOT units could be the reason for this elevated conductivity. First, we confirmed that the synthesis was reproducible synthesis by comparing a typical batch polymerization (~300 mg, PE_2 b1) to a scaled-up 2-gram batch (PE_2 su). Both polymer batches generated high yields (~90%), similar number average molecular weights (M_n) on the order of 5–6 kg/mol according to gel-permeation chromatography (GPC), they were indistinguishable by high-temperature NMR, and had nearly identical elemental compositions. We also used matrix-assisted laser desorption/ionization time-of-flight (MALDI-TOF) mass spectrometry (MS) to characterize different PE_2 batches to elucidate changes in structure within different

polymer batches. The MALDI-TOF spectra of the 300 mg and the 2 g batches of PE_2 confirmed that the two batches were indeed very similar with M_n 6.1 kg/mol and 6.6 kg/mol, respectively (see Figure 1b).

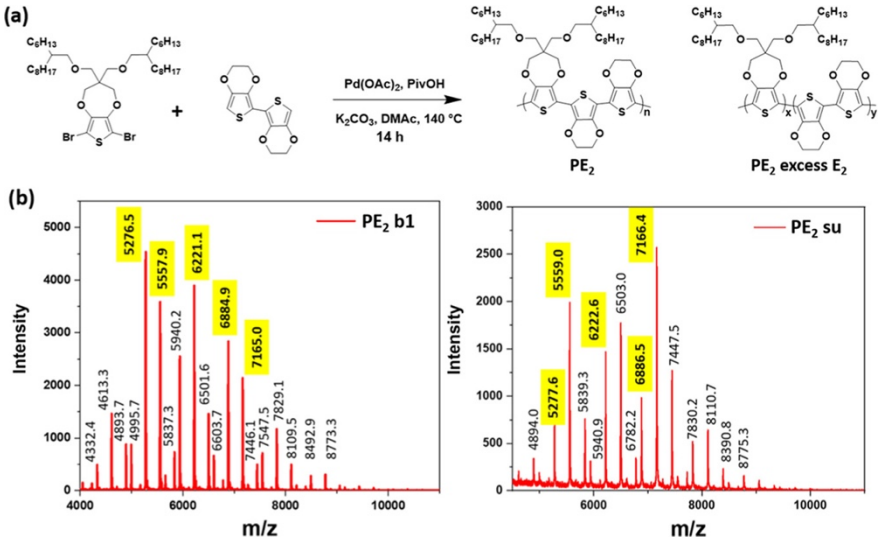

Figure 1. (a) DHAP of PE_2 reaction scheme and (b) MALDI-TOF spectra of two PE_2 batches. Both batches used the standard DHAP protocol and a polymerization temperature of 140 °C but PE_2 b1 was done on a 300 mg scale where as PE_2 su was done on a 2g scale. Adapted from Jones et al. *Macromolecules* 2020, 53, 7253.

Using MALDI-TOF we were also able to study homocoupling defects that can easily go unnoticed because conjugated polymers are commonly characterized via GPC and elemental analysis, two techniques that are not able to provide information on monomer incorporation or end groups. We were able to determined that excess biEDOT is indeed incorporated into PE_2 when using standard direct (hetero)arylation polymerization (DHAP) conditions at high temperatures (≥120 °C) as a result of homocoupling of the biEDOT monomer, which decreases the solubility of the growing polymer chains dramatically resulting in low-molecular-weight polymers (~6 kg/mol). We hypothesize that the high nucleophilicity of biEDOT causes uncontrolled concerted metalation–deprotonation steps in the DHAP catalytic cycle at high temperatures. To improve control of the biEDOT incorporation, we therefore optimized the temperature during the polymerization reaction as well as develop a different polymerization procedure for DHAP where the reaction temperature was ramped-up from room temperature to the target temperature. Manipulation of the DHAP technique, and lowering the reaction temperature, resulted in greater control of biEDOT incorporation resulting in a dominant MALDI peak with precisely five ProDOT units and six biEDOT units. Solid-state conductivity measurements revealed that the polymers with excess biEDOT produced higher values with an average of 200 S/cm. We were able to show that homocoupling defects are

especially sensitive when a biaryl monomer lacking a side chain, such as biEDOT, is incorporated into a polymer as this drastically decreases solubility. This work was published in *Macromolecules* in 2020.

3.2 Synthesis and development of amide-functionalized ProDOT polymers via DHAP

During this grant period we have also developed and synthesized ester, amine, and amide containing ProDOT-derivatives with the ultimate goal of probing effects of incorporating polar substituents and groups with H-bonding capabilities on transport properties. This a relatively unexplored area in the conjugated polymer community due to the synthetic challenges involved but recent studies have shown that the incorporation of H-bonding substituents into the side chains can promote unique self-assembly and macromolecular, which can improve charge transport properties (see Ocheje et al. *Macromolecules* 2018, 51, 1336). Four monomers (1-4 in Figure 2) were successfully synthesized with high yields (>70%) and purity (verified by MS, ^{1}H-NMR, ^{13}C-NMR, and elemental analyses). Our first attempts of making ester and amide containing systems was to synthesize homopolymers using compounds (1) and (2) in Figure 2 with DHAP by varying reaction conditions and ligands. However, despite trying several different conditions, we were not able to obtain soluble polymers. At this point, it is not clear if this is due to aggregation induced by H-bonding from the amides or if the amide substituents are adversely interacting with the palladium catalyst. It is possible that interchain H-bonding through the amide functionality would enhance the packing of copolymers and disrupt chain-solvent interactions. However, palladium catalysts are also used in the cross-coupling of amide and urea starting materials and so they may, therefore, be inhibiting the catalyst from participating in the catalytic cycle.

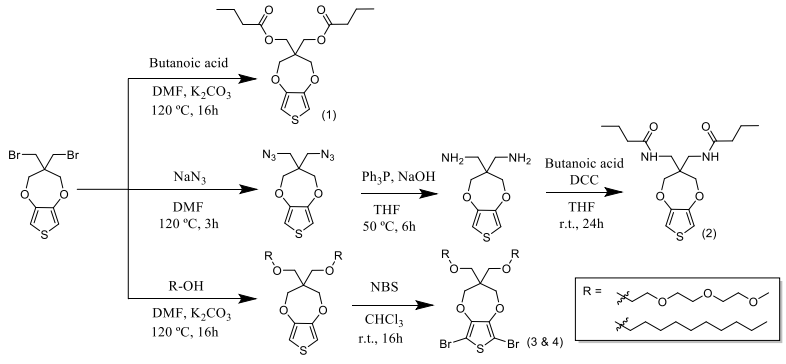

Figure 2. Reaction diagram for the general synthesis of the four monomers evaluated.

To enhance solubility, we instead opted to make copolymers with oligoether and aliphatic derivatized ProDOT comonomers. We successfully synthesized P1, P2, P3, and P4 in Figure 3 (top) with number average molecular weights of 25.5, 22.8, 24.6, 23.9 kg/mol, respectively. These polymers are soluble in chloroform and of high purity as

determined by ^{1}H-NMR and elemental analysis. As shown in Figure 3 (bottom), tracking temperature dependences of amide proton chemical shifts are valuable probes of hydrogen bonding, temperature-dependent loss of structure, and exchange between distinct polymer conformations. Fundamentally, these changes in chemical shift as a function of temperature result from changes in the local magnetic environments of nuclei. This provides strong evidence of H-bonding. This was an exciting result, as this is the first unprotected amide-derivatized ProDOT synthesized by DHAP. Further characterizations of their redox and transport properties are currently underway.

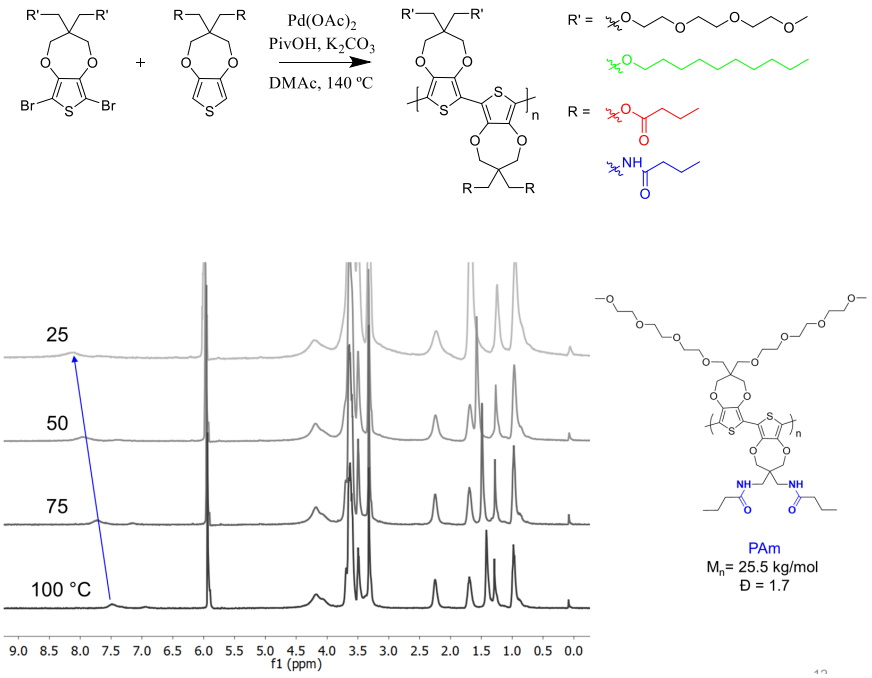

Figure 3. (top) DHAP pathway to yield the four target copolymers with different side chains: black and red **(P1)**, black and blue (**P2**), green and red (**P3**), green and blue (**P4**). (bottom) Variable temperature 1H-NMR experiment for P1 in tetrachloroethylene-d2.

3.3 Attempts for inducing planarity and inter-chain packing

Because planarization, pi-stacking, and charge delocalization are expected to impact the ultimate conductivity, we had proposed to use unfunctionalized thiophene and TT as spacer units in the main chain to extend conjugation further and enhance inter-chain packing. However, these units reduced the solubility to the extent that we were not able to isolate high molecular weight material. In addition, we had proposed to modify some of our higher performing systems, such as PE_2, with linear solubilizing groups rather than branched ones to reduce steric interactions and potential enhance inter-chain packing. Unfortunately, we encountered similar issues here where we were not able to obtain a soluble polymer.

3.4. Backbone effects on conductivity switching in aliphatic PXDOT systems

In an attempt to better understand effect of repeat unit structure on conductivity switching we have varied both the minimally substituted unit as well as the solubilizing unit. To manipulate intra-chain transport, we replaced the solubilizing ProDOT repeat unit with either a fused dioxythiophene (DOTT) with the goal of inducing planarity, or with a 3,4-alkoxythiophene to purposefully twist the backbone out of plane.

First, we compared homopolymers based on ProDOT and acyclic 3,4-alkoxythiophene (Ac) polymers with both linear octyl (Oct) and branched 2-ethylhexyloxy (EH) chains (Figure 4, left). We consistently observed that the ProDOT-based polymers had lower onsets of oxidation, required lower potentials to fully dope, displayed faster doping kinetics, and higher solid-state and electrochemical conductivity (Figure 4, right). The GIWAXS data showed that the Ac polymers had a higher degree of ordering in both the neutral and doped state, as well as as-cast fibril-like topology according to the AFM. By comparing charge capacity and the pseudocapacitance (measured by EIS), we were able to show that more charge carriers were generated in the Ac-polymers but they were not able to transverse the bulk of the film as effectively as in the ProDOT materials. Collectively, the charge transport and morphological characterizations results suggested that the charge transport, especially during electrochemical doping, is compromised in the more ordered materials and that too much ordering and a lack of connection between ordered domains is detrimental for conductivity. This work was published in *J. Mater. Chem.* in 2020.

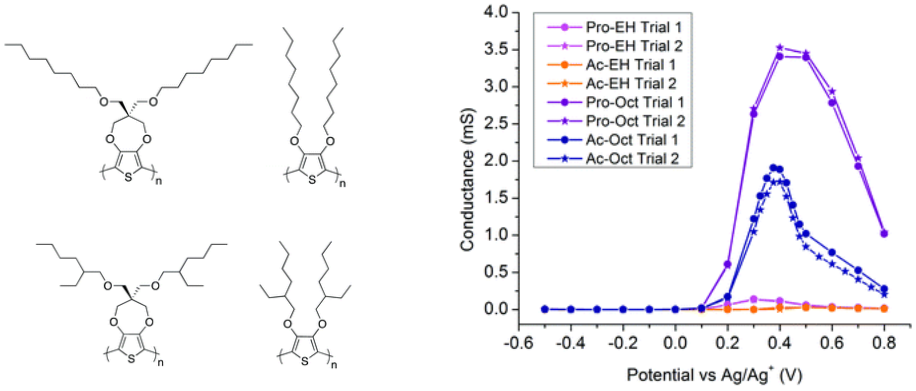

Figure 4. Repeat unit structures and potential-dependent conductance of Pro-EH (magenta), Ac-EH (orange), Pro-Oct (purple), and Ac-Oct (navy blue) on interdigitated electrodes from −0.5 to 0.8 V *vs.* Ag/Ag^+ in 0.5 M $TBAPF_6$/PC. Adapted from Pittelli et al. J. *Mater. Chem. C* 2020, 8, 683.

To probe the effect of planarity, we synthetized and evaluate a series of DOTT-based polymers. In addition to the homopolymer, we compared DOTT copolymerized with either EDOT, dimethyl-substituted ProDOT (DMP), or a bulky neopentyl dioxythiophene

(NeoDOT) unit (Figure 5, left), as our recent research has pointed towards the fact that unsubstituted or minimally substituted spacer units are important for obtaining high conductivity and fast doping kinetics. Using a combination of GIWAXS, XPS, UV-vis-NIR spectroscopy, and in-plane solid-state conductivity measurements, we were able to clearly show that polymers with intermediate degrees of ordering had superior properties (higher electrical conductivity, lower onsets of oxidation, and higher electrochemical conductance) compared to polymers with high relative degrees of ordering. GIWAXS measurements showed that copolymers that demonstrated higher degrees of ordering had larger interchain spacing after the doping process, which resulted in solid-state conductivity values that were lower by orders of magnitude. After doping with F4TCNQ, the microstructure of the more disordered systems was not disrupted, implying that the molecular dopant was able to interact with the polymer matrix more effectively, that charge transfer could occur, and that the generated charge carriers could be effectively delocalized along the backbone with minimal trapping (Figure 5, right). The more highly ordered polymer systems appeared to have a "locked conformation" preventing the ease of oxidation and delocalization of charge carriers. The best performing polymer in this DOTT-family was the one incorporating biEDOT and reached a conductivity of 20 S/cm after chemical doping with F4TCNQ, i.e., an order of magnitude lower than the ProDOT analog. This suggested that while the fused DOTT unit is more planar than ProDOT in absence of side chains, the addition of large solubilizing groups on the DOTT unit seems compromise the charge transport properties. This work was published in *J. Mater. Chem. C* in 2020.

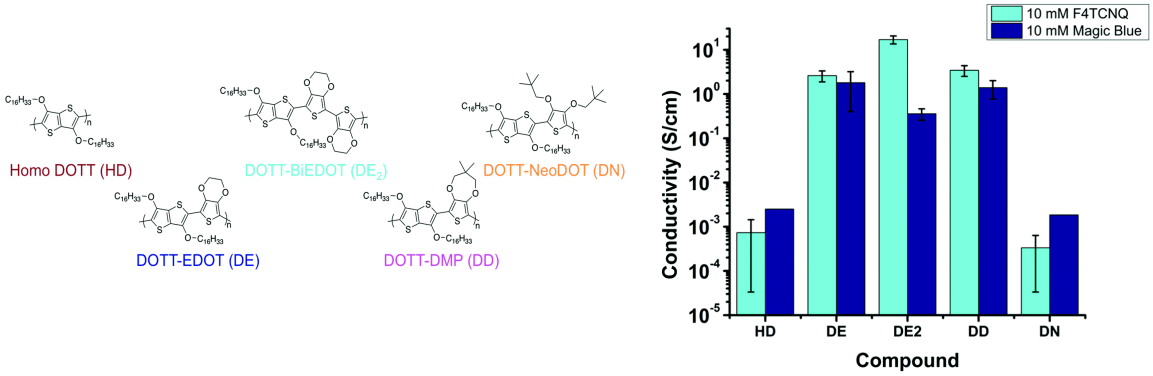

Figure 5. Repeat unit structures and solid-state conductivity values of blade-coated polymer films on glass after exposure to either a 0.01 M Magic Blue or 10 mM M F4TCNQ solution in propylene carbonate for 30 seconds. Adapted from Pittelli et al. *J. Mater. Chem. C* 2020, 8, 7463.

3.5. Side-chain effects on conductivity switching

Traditionally, alkyl side chains are used in the synthesis of organic semiconductors to afford solubility and processability. Appending polar side chains, such as oligoether moieties, has the added benefit of facilitating aqueous redox switchability, which has

attracted much interest from the field of bioelectronics. Side chains can either hinder or promote tight packing of the aromatic backbone, prevent/cause aggregation, and induce torsional backbone order/disorder, which can adversely or favorably affect charge transport over length scales relevant to thin films. For example, it has been shown that the length and placement of linear alkyl side chains can lead to closer packing of the main chain through interdigitation, while the steric bulk introduced by branched chains inhibits this packing.

Results collected in conjunction with the data discussed in Figure 4, provided some insight into how side chains can influence charge transport and switchability. In these dialkoxythiophene and ProDOT-based homopolymers where every repeat unit is functionalized with solubilizing groups, the steric interactions arising from the bulkier branched side chains had a negative impact on both solid-state and electrochemical conductivity, similar to what has been observed in the literature. GIWAXS results suggested that tighter packing of polymer chains due to side chain interactions inhibit oxidation and redox switching. Furthermore, the torsional strain on the backbone caused conformational twisting making the film more difficult to oxidize electrochemically. However, in polymers containing minimally substituted spacer units the side-chain induced effects are not as stark. Comparing the redox behavior of five ProDOT-DMP copolymers with different side chains (Figure 6, left), we observed the length of the side chain influences the onset of bulk conductance and oxidation where polymers with the shortest chains had the lowest onset of oxidation and bulk conductance. At high doping levels, however, there are large differences in the potential dependent conductance trends when we varied the side chains (Figure 6, right). These differences were shown to arise from the relative difference in the amount of delocalized and electrochemically "trapped" charge carriers, which we were able to distinguish form one another using electrochemical impedance spectroscopy. We also evaluated the effect of molecular weight (M_n) on the potential dependent conductivity and solid-state conductivity. Comparing three different M_n batches (104 kg/mol, 69 kg/mol, and 18 kg/mol) of hexyldecyloxy-substituted ProDOT-DMP, we observed no difference in the onset of oxidation and conductance, the current density, conductance magnitude, or conductance contrast. There was a slight difference in the solid-state conductivity where the two higher molecular weight polymers reached a conductivity of around 5 S/cm (unoptimized) after chemical doping with F4TCNQ and the 18 kg/mol batch had a lower conductivity of 0.8 S/cm. According to GIWAXS, the ProDOT-DMP polymers exhibit no long-range order regardless of the choice of side chain, which may partially explain the insensitivity to molecular weight. Compared to the ProDOT homopolymer, these DMP-containing co-polymers exhibit much lower onset of oxidation, three orders of magnitude enhancement in solid-state conductivity, and faster doping kinetics demonstrating the importance of incorporating minimally substituted spacer units. Parts of this work were published in *Chem. Mater.* in 2019.

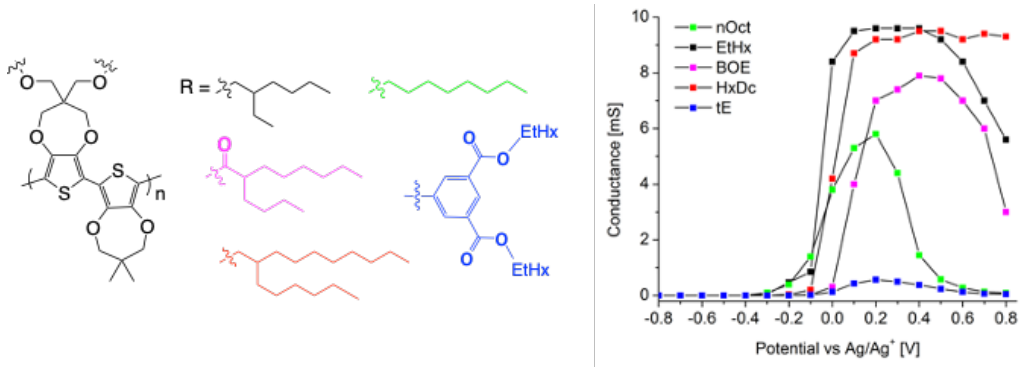

Figure 6. Chemical structures of ProDOT-DMP functionalized with different solubilizing groups and a summary of the potential dependent conductance response of these copolymers in 0.5 M $TBAPF_6$/propylene carbonate. Adapted from Österholm et al. *Chem. Mater.* 2019, 31, 8, 2971.

In a previous ONR funded program we attached polar oligoether chains on the ProDOT units in ProDOT-DMP to enhance polarity and induce aqueous electrolyte compatibility. In addition to being electroactive and stable in salt water, the polymer exhibited a competitive mobility of 0.063 $cm^2\ V^{-1}\ s^{-1}$ and on/off current ratios exceeding 10^5 in an electrochemical transistor set-up and was, at least as of late 2020, the highest performing ProDOT-based transistor material. In this program, wanted to capitalize on the high conductivity observed in PE_2 and combine it with the polarity induced by oligoether chains to create polymers that potentially would have stronger polymer-dopant interactions and therefore higher conductivity. Based on our earlier challenges with functionalizing PE_2 with linear chains, we replaced the linear oligoether chains with branched analogs to ensure solubility (see Figure 7, left). The branched oligoether chains were synthesized in an asymmetric fashion where diethylene glycol (OE2) and triethylene glycol (OE3) are used to generate the side chain branches. We evaluated the two DHAP conditions discussed in conjunction with Figure 1 (i.e., one using standard conditions at 140 °C and then another starting at 30 °C, followed by a temperature ramp-up of 10 °C every 5 min until a final temperature of 90 °C was reached) that gave us two polymers one with a M_n of 12 kg/mol (140 °C, yield 40%, PE_2-biOE2OE3(L)) and another with a M_n of 20 kg/mol (temperature ramp, yield 85 %, %, PE_2-biOE2OE3(H)). These two polymers demonstrated a significant molecular-weight dependent solubility, processability, and solid-state conductivity after oxidative doping. PE_2-biOE2OE3(L) can be dissolved in acetone at a concentration of >30 mg mL^{-1} and processed into films that achieved an average solid-state conductivity of 55 ± 3 S cm^{-1}. In contrast, PE_2-biOE2OE3(H) was only soluble in chlorinated solvents, but yielded films with a higher average solid-state conductivity of 430 ± 60 S cm^{-1}. To date, this is the highest solid-state conductivity for a CP incorporating ProDOT and/or OE-functionalization that has been reported. This work was recently published in *Adv. Funct. Mater.* in June 2021.

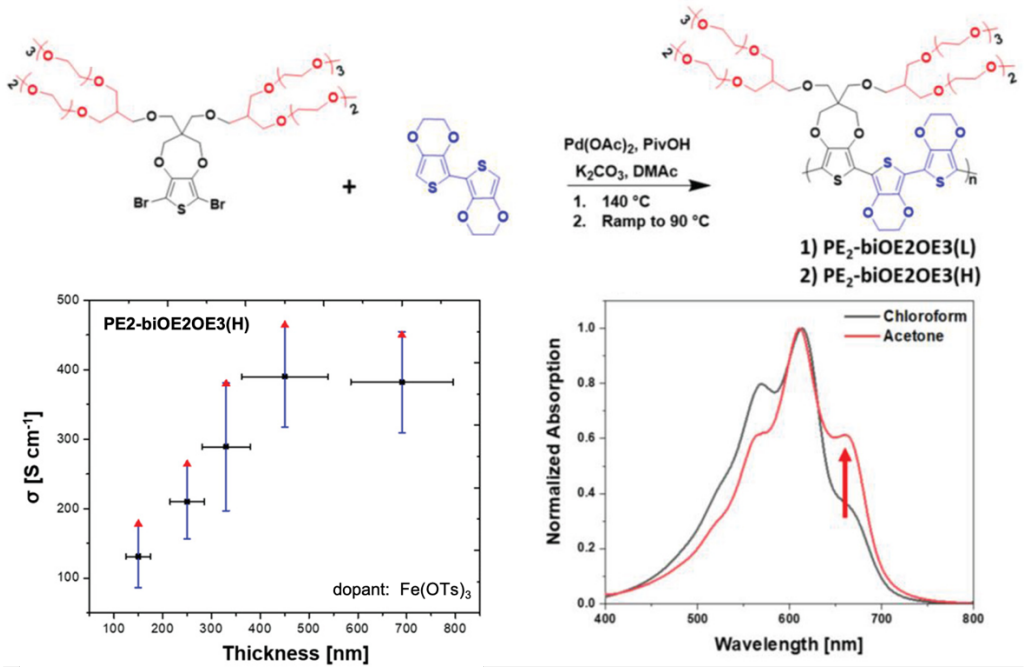

Figure 7. (top) PE_2-biOE2OE3 synthetic scheme. (bottom left) Average solid-state conductivities of PE_2-biOE2OE3(H) films of varying thickness. Red data points are the maximum conductivities measured. All samples are doped using a $Fe(OTs)_3$ solution in isopropanol. The error bars represent the standard deviation. (bottom right) Normalized UV–vis absorption spectra of PE_2-biOE2OE3(L) in dilute solution at room temperature treated with hydrazine (chloroform in black and acetone in red). The red arrow in (c) indicates increased J aggregation in acetone relative to chloroform. Adapted from Jones et al. in *Adv. Funct. Mater.* 2021, 2102688.

3.6. Incorporating XDOT systems into switchable devices

During this grant period we have had the opportunity to collaborate with both federal and academic teams. A collaboration with the Navy Research Laboratory (Jeff Long and Megan Sassin) resulted in flexible supercapacitors incorporating hexyldecyloxy-functionalized ProDOT-DMP as a nanoscale conformal coating on macroscale high-surface area carbon fiber paper substrates. Using the sequential deposition procedure, up to 39 wt % polymer loading could be achieved using the porous carbon fiber paper resulting in a >50x enhancement of the areal capacitance of the carbon paper (see Figure 8). As for the polymer, coating it on the 3D carbon substrate resulted in a 120x increase in the geometric capacitance compared to an analogous 2D planar film. Furthermore, by keeping the polymer coating conformal to the carbon surfaces, the high-rate character associated with the copolymer was retained; redox couples are still evident at scan rates up to 50 mVs^{-1}, which is fast a 200 μm-thick electrode. We showed that area- and volume-normalized metrics generally tracked with polymer loading, and that the polymer domains in the CFP can serve as a glue to laminate multiple sheets of polymer-coated CFP via hot-pressing,

forming a unitized electrode with a reduced void volume and therefore significantly enhanced volumetric charge storage. Normalizing the current to electrode footprint reveals an area-normalized capacity of 0.11 mAh cm^{-2} (0.25 F cm^{-2}) for the hot-pressed electrodes compared to 0.06 mAh cm^{-2} (0.1 F cm^{-2}) for electrodes that had not been hot-pressed as this additional step allowed us to double the mass-per-area. We also evaluated the cycle life of these devices and found that 91% of the capacity is retained over 10,000 cycles. This work was published in 2020 in *ACS Appl. Polym. Mater*.

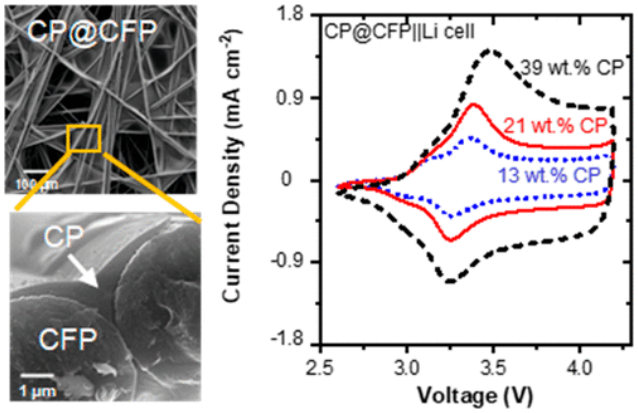

Figure 8. (left) Scanning electron micrographs of ProDOT-DMP coated CFP. (right) CVs of ProDOT-DMP@CFP/Li cells with varying polymer loading. Adapted from Sassin et al. *ACS Appl. Polym. Mater.* 2020, 2, 8, 3234.

Working together with the Mirotznik group at the University of Delaware, we have incorporated PE_2 into switchable antenna structures and show that a significant change in transmission can be achieved at high frequencies (GHz). Based on their modelling and calculations done at UD, three different applications were proposed: (i) a dipole antenna with ON/OFF switchable ends, (ii) an overlapping cross FSS, and (iii) a microstrip transmission line pattern separated by a switchable dielectric material. We ended up focusing our efforts on the switchable dipole antenna. First, we evaluated the lateral conductivity of the CP films using the patterned electrode configurations where we varied the distance between the two electrodes from 5 to 15 mm. These experiments showed that PE_2 was a promising candidate that could readily switch over 15 mm without an underlying conductor (see Figure 9, top left). Traditionally the performance of antennas depends on the geometry, size, and configuration. To dynamically modify their frequency of operation reversibly and on demand, most tunable antennas use an internal electrical switching mechanism to change the physical and electrical dimensions. We were able to demonstrate that we can use PE_2 as a switch in a tunable half-wave dipole antenna using a low DC voltage to make the antenna tunable in the ultra-high frequency range, more specifically in the 1-5 GHz range (see schematic in Figure 9, top right). Simulation data of this new type of tunable dipole antenna show that its feasibility depends on the maximum achievable relative conductivity contrast between the ON and OFF state, its long-range (millimeter

range) switchability and that a conductivity contrast from 10^{-4} S/cm to 1 S/cm is sufficient to tune the antenna, which several of the CPs evaluated in this program can achieve (Figure 12, bottom left). We designed two different proof-of-concept devices, one solid-state device where the PE_2 was either in its insulating or its chemically doped state, and one electrochemical device where the conductivity of the PE_2 was user-controlled. Figure 12 (bottom right) shows the measured reflection coefficient for the antenna. The red curves show the antenna response when the PE_2 film is in its neutral state, and the blue curves when it is in its doped state. From these results we could clearly demonstrate that the resonance frequency of the antenna could be tuned by the switch. In the electrochemical switch, however, the conductivity of the electrolyte interfered so the switching contrast was slightly compromised. Moving forward, the electrolyte thickness and conductivity can be optimized to improve the performance of the electrochemical switch. This work is in draft form and is expected to be submitted to Nature Mater. in September 2021.

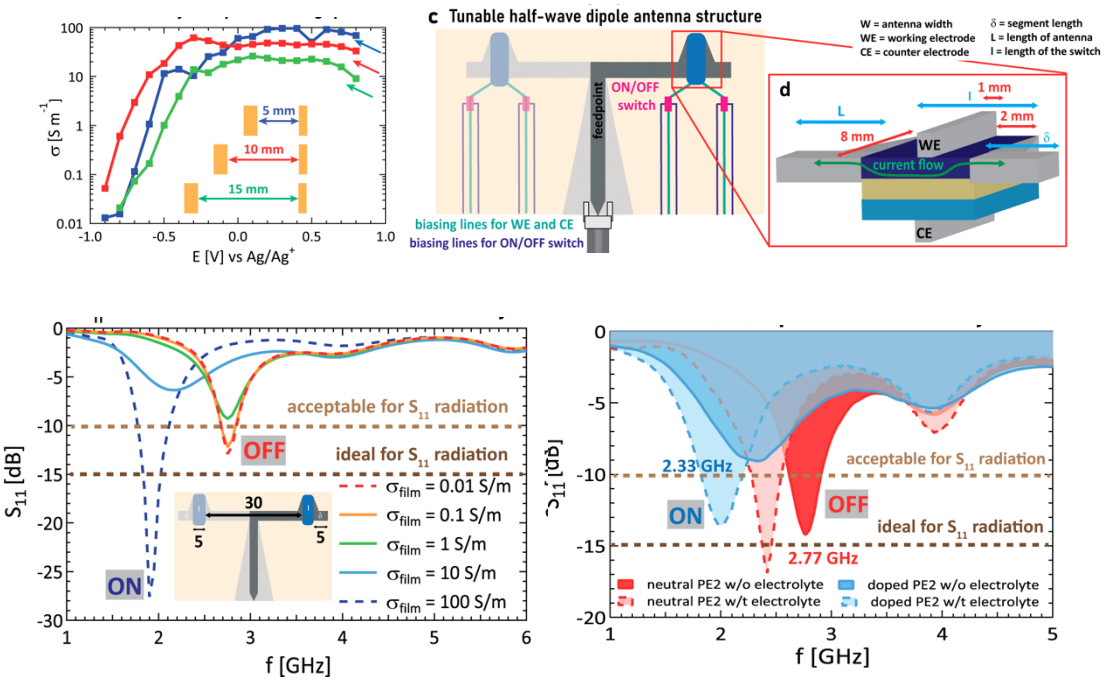

Figure 9. (top left) Conductivity contrast PE_2 film on customized patterned electrodes with different gap sizes. (top right) Schematic representation of the tunable half-wave dipole antenna structure with biasing lines and a schematic of the design of the electrical PE_2 switch. (bottom left) Simulated reflection coefficient for the antennas with PE_2 switches of varying conductivity. (bottom right) Measured reflection coefficients for antennas in the OFF (red) and ON (blue) states with (solid lines) and without (dashed lines) the presence of electrolyte.

4. Concluding remarks

In this program, we have designed, synthesized, solution processed and characterized multiple families of electron-rich, redox active, conjugated polymers that undergo facile electrochemical switching. We have explored direct heteroarylation polymerization methods, yielding well-characterized polymer structures of known repeat units and degrees of polymerization. In multiple cases, we have demonstrated structurally controlled electronic conductivity for oxidatively doped complexes of these polymers, and monitored conductivity changes as a function of electrochemical potential. Both main chain and side chain effects are elucidated, showing the subtle and complicated interplay of these variables and how these ultimately affect processing of polymer solutions and aggregates. Finally, we have incorporated these polymers into electrochemically switchable charge storage and conducting element devices. Supercapacitors based on our polymers were found to retain over 90 % of their charge capacity capacity over 10,000 cycles, and we could clearly demonstrate that the resonance frequency of an RF antenna could be tuned by the switch.

Publications acknowledging funding from N00014-18-1-2222

Österholm, A. M.; Ponder, J. F.; De Keersmaecker, M.; Shen, D. E.; Reynolds, J. R. "Disentangling Redox Properties and Capacitance in Solution-Processed Conjugated Polymers" *Chem. Mater.* 2019, 31, 8, 2971–2982

Keersmaecker, M., Reynolds, J. R. "Simple Interface Modification of Electroactive Polymer Film Electrodes" *ACS Appl. Mater. Interfaces* 2019, 11, 47131.

Sassin, M. B.; Hoffmaster, A. N.; Österholm, A. M.; Lo, C. K.; Reynolds, J. R.; Long, J. W. "Integrating Solution-Processable Conducting Polymers in Carbon Fiber Paper: Scalable 3D Electrodes for Redox-Based Supercapacitors" *ACS Appl. Polym. Mater.* 2020, 2, 3234.

Pittelli, S. L.; De Keersmaecker, M., Ponder, J. F.; Österholm, A. M.; Ochieng, M. A.; Reynolds, J. R. J. "Structural effects on the charge transport properties of chemically and electrochemically doped dioxythiophene polymers" *J. Mater. Chem. C* 2020, 8, 683.

Pittelli, S. L.; Gregory, S., Ponder, J. F.; Yee, S. K.; Reynolds, J. R. "Inducing planarity in redox-active conjugated polymers with solubilizing 3,6-dialkoxy-thieno[3,2-*b*]thiophenes (DOTTs) for redox and solid-state conductivity applications" *J. Mater. Chem. C* 2020, 8, 7463.

Jones, A. L.; De Keersmaecker, M., Pelse, I.; Reynolds, J. R. "Curious Case of BiEDOT: MALDI-TOF Mass Spectrometry Reveals Unbalanced Monomer Incorporation with Direct (Hetero)arylation Polymerization" *Macromolecules* 2020, 53, 7253.